In Situ Analysis of Volatiles Obtained from the Catalytic Cracking of Polyethylene

NATHAN D. HESSE, RONG LIN, EDOUARD BONNET, JESSE COOPER III, ROBERT L. WHITE

Department of Chemistry and Biochemistry, University of Oklahoma, Norman, Oklahoma 73019

Received 6 November 2000; accepted 20 April 2001

ABSTRACT: The effects of the solid-acid-catalyst pore size and acidity on polyethylene catalytic cracking were examined with a comparison of the temperature-dependent volatile-product-slate changes when the polymer was cracked with HZSM-5 and HY zeolites and the protonated form of MCM-41. Volatile-product distributions depended on the catalyst acidity and pore size. With HZSM-5, paraffins were detected initially, and olefins were produced at somewhat higher temperatures. Aromatics were formed at temperatures 30–40°C higher than those required for olefin production. Small olefins (C_3–C_5) were the most abundant products when HZSM-5 and MCM-41 catalysts were employed for cracking polyethylene. In contrast, cracking with HY produced primarily paraffin volatile products (C_4–C_8). HY pores were large enough and the acid sites were strong enough to promote disproportionation reactions, which led to the formation of volatile paraffins. Compared with the other catalysts, HZSM-5 with its smaller pores inhibited residue formation and facilitated the production of small alkyl aromatics. Volatile-product variations could be rationalized by a consideration of the combined effects of catalyst acidity and pore size on carbenium ion reaction pathways. © 2001 John Wiley & Sons, Inc. J Appl Polym Sci 82: 3118–3125, 2001

Key words: catalytic cracking; polyethylene (PE); HZSM-5; HY; MCM-41; recycling; thermal properties

INTRODUCTION

A variety of plastic-waste recycling methods have been established, and new recycling approaches are being developed to avoid placing polymers into landfills. One approach to plastic-waste recycling, known as *tertiary recycling*, consists of decomposing plastics into useful chemicals or fuels. Catalytic cracking is potentially a very useful tertiary recycling tool. Previous studies of the catalytic cracking of polyethylene (PE), which constitutes about 47 wt % of the total plastic waste in the United States,[1] have shown that the molecular weight range of volatile products generated by heating this polymer can be greatly restricted with solid acid catalysts.[2–16]

Although a wide variety of catalysts have been employed to crack PE, zeolites have proven particularly effective. For example, Garforth et al.[2] reported that activation energies measured when PE was catalytically cracked by HZSM-5, HY, and MCM-41 were much lower than when no catalyst was present. They concluded that HZSM-5 and HY had similar activities and that both of these zeolites were more effective than MCM-41. Manos et al.[3,4] found that the catalytic cracking of PE by HZSM-5 and HY was effective in producing gasoline-size hydrocarbons in a laboratory semibatch reactor. Mordi et al.[7] reported that H-theta-1 and H-mordenite zeolites, with pore diameters comparable to those for HZSM-5 and HY, were rela-

Correspondence to: R. L. White (rlwhite@chemdept.chem.ou.edu).

Journal of Applied Polymer Science, Vol. 82, 3118–3125 (2001)

tively ineffective in producing gasoline-size hydrocarbons from PE cracking. Clearly, the catalyst pore size and acidity are important factors in polymer catalytic cracking.

Most PE catalytic cracking studies have been performed by the heating of reactor vessels containing catalyst and polymer and the subsequent collection and analysis of the products. This batch-processing approach provides no information regarding the order in which products form. In addition, if sealed reaction vessels are employed, initial reaction products may react with catalysts to form secondary products. We have developed a repetitive-injection gas chromatography/mass spectrometry (GC/MS) evolved gas analyzer that facilitates the separation, identification, and quantification of volatiles generated by the heating of solid samples.[17] With this apparatus, product trapping is not required. Instead, volatile products are removed from catalysts with an inert purge gas and then analyzed online. This article describes results obtained with this apparatus to monitor the temperature dependence of volatile-product slates obtained by the cracking of PE with HZSM-5, HY, and MCM-41. Because these three acid catalysts possess different acid strengths and pore structures, information regarding the effects of pore structure and acid strength on cracking processes can be obtained by comparisons of volatile-product evolution profiles.

EXPERIMENTAL

Materials

PE with an average molecular weight of 80,000 was purchased from Aldrich Chemical Co. (Milwaukee, WI). HZSM-5 was prepared by following previously described procedures with tetrapropylammonium bromide as a template.[18] ZSM-5 powder was washed with deionized water for the removal of bromide ions and then dried at 110°C for several hours. Sodium was removed from the catalyst by ion exchange with a 0.1*M* ammonium nitrate solution, and the catalyst was then calcined at 550°C for 3 h. An electron microprobe analysis of the catalyst revealed that the Al_2O_3 content was about 5 wt %. The MFI-type crystal structure (5.3 × 5.6 Å and 5.1 × 5.5 Å intersecting channels) of ZSM-5 was confirmed by X-ray powder diffraction.

Mesoporous (15–150-Å pore sizes) MCM-41 was synthesized with procedures described in the literature; dodecyltrimethyl-ammonium bromide and tetramethyl-ammonium hydroxide were used as templates.[19–22] The resulting powder was ion-exchanged with a 0.1*M* ammonium nitrate solution for the removal of alkali ions and then calcined for 6 h at 540°C. An electron microprobe analysis revealed that the Al_2O_3 content of this catalyst was about 17 wt %. The hexagonal crystal structure of MCM-41 was confirmed by X-ray powder diffraction.

The HY catalyst (7.4-Å channel diameter) was derived from NaY (Y-54), which was obtained from Union Carbide (Danbury, CT). Sodium was removed from the catalyst by ion exchange with a 0.1*M* ammonium nitrate solution, and the catalyst was then calcined at 550°C for 3 h. The Al_2O_3 content in this catalyst was reportedly 19 wt %.

Measurements

The acidic properties of the solid acid catalysts were characterized by the temperature-programmed desorption (TPD) of ammonia. A fixed-bed microreactor built in our laboratory was used to generate ammonia TPD curves.[23] Approximately 100-mg samples of each catalyst were calcined *in situ* at 600°C (HZSM-5 at 550°C) with a 25 mL/min air flow for 2 h. After calcination, catalyst samples were allowed to cool to 100°C under a helium purge (25 mL/min). After cooling, anhydrous ammonia (Airgas, Radnor, PA) was passed through catalyst samples. Excess ammonia was then flushed with helium (25 mL/min) until ammonia could no longer be detected by a Hewlett–Packard (Palo Alto, CA) 5988A mass spectrometer. Ammonia was desorbed by the heating of the reactor furnace from 100 to 700°C at a rate of 10°C/min. Ammonia TPD curves were derived from temperature-dependent *m/z* 17 ion signals after correction for water-ionization contributions.

PE/catalyst samples were prepared by the combination of about 10 wt % PE ($<150\mu$m) with catalyst powders ($<150\mu$m). Thermal analyses of PE/catalyst mixtures were accomplished by the heating of samples at a rate of 2°C/min in a tube furnace with the repetitive analysis of the helium purge gas effluent by GC/MS. The apparatus used to obtain repetitive evolved gas chromatograms is described in detail elsewhere.[17] For each separation, the GC oven temperature ramp began with a 0.5-min isothermal period at −20°C followed by heating at a rate of 50°C/min to 150°C. A 10-m, 0.25-mm-inner-diameter DB-1 capillary GC col-

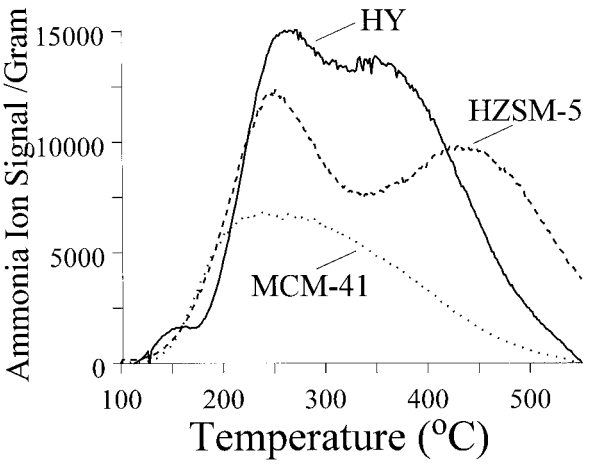

Figure 1 Ammonia TPD curves.

umn with a 0.25-μm stationary phase thickness and a 2 mL/min helium carrier gas flow rate were employed for separations. The amount of residue remaining on the catalyst surfaces after heating to 600°C in helium was determined by oxidative thermogravimetry with a DuPont model 951 thermogravimetric analyzer (Wilmington, DE).

RESULTS

Ammonia TPD curves for the three acid catalysts are shown in Figure 1. The normalized ammonia *m/z* 17 ion signals (*y* axis) plotted in Figure 1 denote relative ammonia desorption rates. On the basis of the curves in Figure 1, HY had the most acid sites, and MCM-41 had the fewest. The HZSM-5 TPD curve extends to higher temperatures than those for the other catalysts, indicating that HZSM-5 contained a greater fraction of higher acid-strength sites.

Figure 2 shows repetitive-injection chromatograms obtained during the heating of PE/catalyst samples at 2°C/min in a helium atmosphere. The tic marks on the *x* axes in Figure 2 denote PE/catalyst sample temperatures at which evolved gases were injected into the gas chromatograph. Purge gas effluent was analyzed at 5-min intervals, which corresponded to 10°C sample temperature increments. Figure 2 shows that the temperature range over which volatiles were produced depended on the choice of the cracking catalyst. The maximum volatile-product elution rate for the PE/HY sample occurred at the lowest temperature (220°C), followed by the PE/MCM-41 (260°C), and PE/HZSM-5 (280°C) samples. Although the maximum volatile-product evolution rate for the PE/HZSM-5 sample occurred at 280°C, products were detected at as low as 150°C. After a comparison of the shapes of individual chromatograms in Figure 2(a), it is apparent that volatile-product distributions changed significantly for the PE/HZSM-5 sample above 290°C. The dominant volatile species detected above 310°C were found to be alkyl aromatics. Similar variations are apparent in the PE/HY chromatograms [Fig. 2(b)]. Although volatile-product slates for the PE/MCM-41 sample also changed with temperature, no alkyl aromatic species were detected in the repetitive-injection chromatograms for this sample.

Chromatograms obtained during the heating of the three PE/catalyst samples show catalyst-dependent differences in volatile-product distributions. Figure 3 shows the gas chromatograms obtained at temperatures corresponding to the maximum volatile-product evolution rates for each PE/catalyst sample. Figure 3 clearly shows that relative hydrocarbon product yields depended on which catalyst was employed. For the PE/HZSM-5 sample [Fig. 3(a)], many isomeric hydrocarbons were detected, most of which were low molecular weight substances with short retention

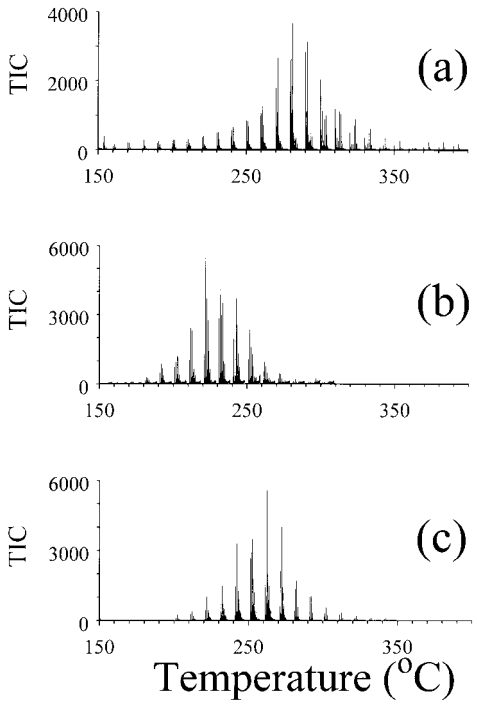

Figure 2 Evolved gas chromatograms obtained by repetitive-injection GC/MS for (a) PE/HZSM-5, (b) PE/HY, and (c) PE/MCM-41 samples.

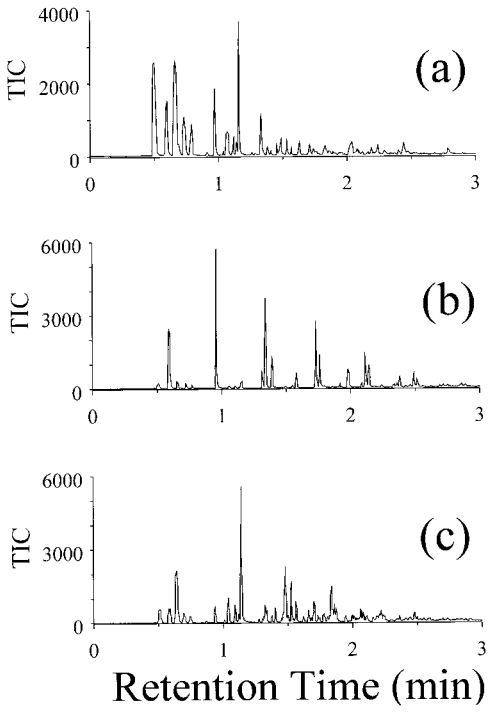

Figure 3 GC/MS chromatograms obtained at sample temperatures corresponding to maximum volatile-product evolution for (a) PE/HZSM-5 (280°C), (b) PE/HY (220°C), and (c) PE/MCM-41 (260°C) samples.

times. Volatile-product diversity is less evident in the PE/HY chromatogram [Fig. 3(b)]. The volatile-product slate generated by the heating of the PE/MCM-41 sample [Fig. 3(c)] was similar to that obtained for the PE/HZSM-5 sample, except that low molecular weight products were not as abundant.

The chromatographic resolution exhibited in Figure 3 was typical of all of the chromatograms obtained during analysis and was sufficient to permit the calculation of species-specific evolution profiles. Figure 4 shows species-specific evolution profiles calculated for paraffin, olefin, and alkyl aromatic volatile products formed by the heating of the PE/HZSM-5 sample. We calculated integrated total ion current (TIC) values by taking the sum of the TIC chromatographic peak areas for all species detected at each temperature that had the indicated number of carbon atoms. The numbers in parentheses denote the number of isomers detected. The volatile-product slates for the PE/HZSM-5 sample show that C_3–C_5 hydrocarbons were the dominant species formed. The temperature corresponding to the maximum paraffin and olefin evolution rates was 280°C [Fig. 4(a,b)], whereas alkyl aromatic evolution maximized at 310°C [Fig. 4(c)]. Below 200°C, volatile-product mixtures were composed entirely of paraffins [Fig. 4(a)]. Mass spectra for paraffin products were consistent with branched-chain rather than straight-chain structures. The only C_4 and C_5 paraffins detected were isobutane and isopentane. Above 200°C, many different olefin isomers were detected in volatile mixtures [Fig. 4(b)]. In addition to paraffin and olefin products, substantial quantities of alkyl aromatics were detected for the PE/HZSM-5 sample. Figure 4(c) shows that aromatics with C_1–C_4 alkyl groups were detected and that C_2-substituted aromatics (xylenes and possibly ethyl benzene) were the dominant aromatic products.

Species-specific evolution profiles for the PE/HY sample are shown in Figure 5. Unlike for PE/HZSM-5, volatile mixtures were primarily composed of C_4–C_8 paraffin rather than olefin products. Evolution profiles for paraffins [Fig. 5(a)] and olefins [Fig. 5(b)] had similar shapes, with maximum evolution rates occurring at 230–240°C. Like the paraffin evolution profiles for the PE/HZSM-5 sample, isobutane and isopentane were significant paraffin products, and no straight-chain isomers were detected. Alkyl aromatic evolution rates maximized at 260–270°C

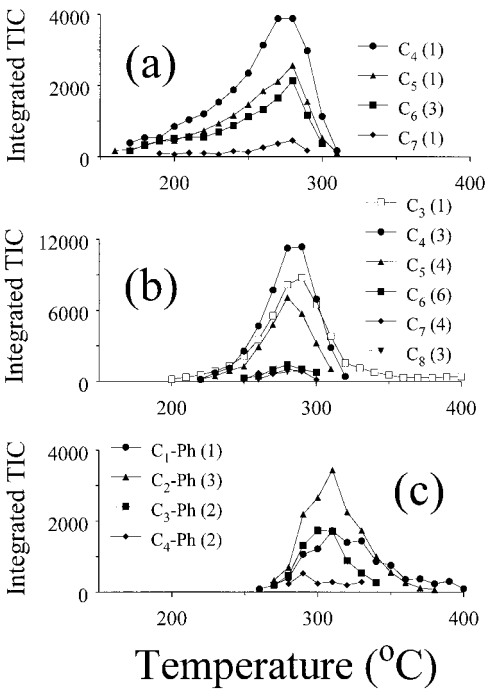

Figure 4 Species-specific evolution profiles of (a) paraffin, (b) olefin, and (c) alkyl aromatic products obtained when a PE/HZSM-5 sample was heated.

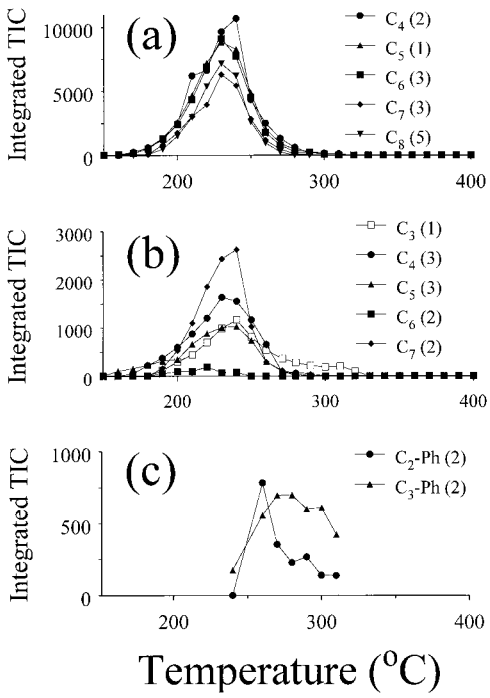

Figure 5 Species-specific evolution profiles of (a) paraffin, (b) olefin, and (c) alkyl aromatic products obtained when a PE/HY sample was heated.

for the PE/HY sample. Alkyl aromatic yields for the PE/HY sample were much lower than for the PE/HZSM-5 sample [Fig. 5(c)].

Species-specific evolution profiles for the PE/MCM-41 sample are shown in Figure 6. As for the PE/HZSM-5 sample, olefin yields were much greater than paraffin yields for the PE/MCM-41 sample. Paraffin evolution profiles in Figure 6(a) mostly represent single isomers. In contrast, many olefin isomeric species were detected [Fig. 6(b)]. C_4–C_6 olefins comprised the largest fraction of volatile mixtures. Unlike for the PE/HZSM-5 sample, propene was a minor volatile product. Alkyl aromatic products were not detected for this sample.

After the samples were heated to 600°C in flowing helium, the amount of carbonaceous residue contained in each sample was measured by thermooxidative weight loss. Oxidizable residue remaining on the PE/HZSM-5 sample was about 3% of the initial polymer mass. Residues on the PE/HY and PE/MCM-41 samples were 9 and 6% of the initial polymer mass, respectively. The lower amount of residue found on the HZSM-5 sample is consistent with the hypothesis that smaller ZSM-5 pores restrict the formation of large unsaturated species believed to be precursors of residue accumulation. The HY sample contained the largest amount of residue, which is consistent with the high volatile paraffin yield.

DISCUSSION

Catalytic cracking mechanisms were solely responsible for the observed product slates because all volatile products were detected at temperatures below those at which thermal cracking could generate volatiles. Volatile products derived from cracking PE with solid acid catalysts can be rationalized by carbenium ion mechanisms. Under steady-state conditions, hydrocarbon cracking processes that yield volatile products can be represented by initiation, disproportionation, β-scission, and termination reactions.[24,25] Initiation involves the protolysis of PE with Brönsted acid sites (H^+S^-) to yield paraffins and surface carbenium ions:

$$C_nH_{2n+2} + H^+S^- \rightarrow C_mH_{2m+2} + C_{n-m}H^+_{2(n-m)+1}S^-$$

Propagation reactions involve disproportionation between feed molecules and surface carbenium ions to yield paraffins:

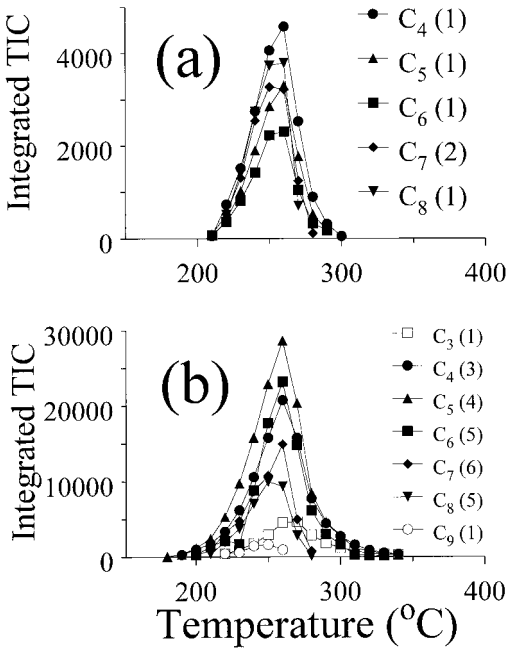

Figure 6 Species-specific evolution profiles of (a) paraffin and (b) olefin products obtained when a PE/MCM-41 sample was heated.

$$C_nH_{2n+2} + C_mH^+_{2m+1}S^- \rightarrow C_{m+x}H_{2(m+x)+2} + C_{n-x}H^+_{2(n-x)+1}S^-$$

When a surface carbenium ion undergoes β-scission to form olefin products, smaller carbenium ions are left on the catalyst surface:

$$C_nH^+_{2n+1}S^- \rightarrow C_xH_{2x} + C_{n-x}H^+_{2(n-x)+1}S^-$$

When sufficiently small, olefins may desorb from catalyst surfaces. Surface olefins may also be protonated to form new carbenium ions. Termination reactions involve the destruction of surface carbenium ions. For example, surface carbenium ions may desorb to produce olefins and regenerate Brönsted acid sites:

$$C_nH^+_{2n+1}S^- \rightarrow C_nH_{2n} + H^+S^-$$

These chain reactions describe how paraffin and olefin cracking products are formed but do not explain residue or aromatic product formation. Like the other reactions, aromatic and coke-forming reactions involve surface carbenium ions.[24,25] Carbenium ion thermal cracking can result in olefin ions, which may undergo dehydrogenation and cyclization reactions that are suspected to be the source of aromatic products from straight-chain paraffin feeds. When unsaturated ions are protonated, di-ions are produced. Doubly charged ions can also be formed by disproportionation reactions between adjacent surface carbenium ions. Multiply charged ions are strongly bound to surface conjugate base sites and are less likely to participate in reactions with feed than singly charged carbenium ions. Consequently, catalyst sites occupied by polyions are unavailable for further reaction. Catalyst acidity and pore size dictate the relative rates of protolysis, disproportionation, β-scission, and termination reactions, which determine the abundance of volatile paraffin, olefin, aromatic, and nonvolatile hydrocarbon products.

Table I lists the total relative yields of paraffin, olefin, and alkyl aromatic volatile products detected for each of the three PE/catalyst samples. Semiquantitative yields were obtained by the integration of all GC/MS peaks in each repetitive-injection chromatogram obtained during PE cracking and the summation of peak areas for each of the three structure classes. The relative yields of paraffins and olefins were heavily dependent on the type of catalyst used for cracking.

Table I Volatile Product Yields

	Total Volatiles[a] (%)		
Catalyst	Paraffins	Olefins	Aromatics
HZSM-5	24.2	60.3	15.5
HY	83.2	14.2	2.6
MCM-41	13.3	86.7	—

[a] Calculated from integrated total-ion current chromatographic peak areas.

MCM-41 had the fewest acid sites and lacked high-acid-strength sites. The high olefin yield for the PE/MCM-41 sample suggests that β-scission dominated PE cracking reactions for this sample. To a lesser degree, olefins also dominated the volatile-product slate detected when PE was cracked by HZSM-5, which had significantly more acid sites and a larger fraction of high-acidity sites compared with MCM-41. In contrast, paraffins dominated the volatile-product slate detected for the PE/HY sample. HY had the largest number of acid sites but did not have as many strong acid sites as HZSM-5. The large discrepancy in the paraffin/olefin ratio detected for the PE/HZSM-5 and PE/HY samples and the trend in maximum evolution temperatures (HY $<$ MCM-41 $<$ HZSM-5) cannot be explained by differences in acidity alone.

The MCM-41 catalyst pores were much larger than those in either the HZSM-5 or HY catalysts. Consequently, the MCM-41 catalyst exhibited the least steric hindrance for disproportionation reactions that yielded paraffins. The low paraffin/olefin ratio for the PE/MCM-41 volatile-product slate suggests that disproportionation reactions were not favored in catalytic reactions despite the large pore size. HZSM-5 and HY catalysts, which have much smaller pore sizes, formed paraffins in larger yields. Thus, differences in the paraffin/olefin ratio for the three PE/catalyst samples cannot be explained solely by pore size considerations.

Disproportionation reaction rates depend on carbenium ion reactivities, which are determined by catalyst-site acid strength. Carbenium ions produced at strong acid sites are less likely to undergo β-scission or desorption.[24,25] Solely on the basis of acid-strength considerations, disproportionation reactions should have been most fa-

vored for the PE/HZSM-5 sample. However, the largest paraffin/olefin ratio was detected for the PE/HY sample. Compared with HY, HZSM-5 with its smaller pores inhibited bimolecular disproportionation reactions. In contrast, the low paraffin/olefin volatile-product ratio for the PE/MCM-41 sample was likely due to the low acidity of the catalyst. Although the MCM-41 pore size was large enough to facilitate disproportionation, catalyst-site acidity was too low for this reaction pathway to be dominant. The low-temperature (<200°C) paraffin yield for the PE/HZSM-5 sample likely resulted from reactions catalyzed by high-acid-strength sites. High-acid-strength sites more readily deactivate. Deactivation of the high-acid-strength sites occurs by the formation of nonreactive residues inside the HZSM-5 pores. Pore blocking by these residues would decrease the reaction volume available for disproportionation, which would further reduce paraffin/olefin ratios.

Aromatic products were detected at temperatures above those at which paraffin and olefin evolutions maximized (Figs. 4 and 5). The shift in alkyl aromatic evolution profiles to higher temperatures relative to paraffins and olefins is consistent with a mechanism in which unsaturated surface ions are precursors for alkyl aromatic formation.[24,25]

Alkyl aromatic yields decreased in the order PE/HZSM-5 > PE/HY > PE/MCM-41, which follows a trend in increasing pore size. Steric restrictions on reaction volume afforded by HY and HZSM-5 promoted aromatic ring formation from conjugated unsaturated polymer segments. The smaller pore HZSM-5 was significantly more effective at forming alkyl aromatics than HY.

Unsaturated residue formed during catalytic reactions that produced paraffins and olefins was the source of alkyl aromatics and nonvolatile residue. When HZSM-5 catalyst was employed, aromatic alkyl chain sizes were restricted to C_4 or smaller. The pores of HZSM-5 were large enough to allow the formation of small alkyl aromatics by cyclization and dehydrogenation of surface species, but the formation of fused unsaturated coke precursors was inhibited. Unlike HZSM-5, HY with its larger pores facilitated the formation of larger, nonvolatile unsaturated coke precursors. After heating, the PE/HY sample contained three times the amount of residue that the PE/HZSM-5 sample had. No aromatic products were detected when the PE/MCM-41 sample was heated. Cyclization reactions were not facilitated within the larger MCM-41 pores. Even though the MCM-41 pore size was much larger than the HY pore size, the amount of oxidizable residue remaining on the MCM-41 catalyst was substantially less than that detected on the HY catalyst.

The PE/HZSM-5 volatile-product slates described here are consistent with our previous work.[8] PE catalytic cracking product yields obtained with fluidized-bed and semibatch reactors with HZSM-5, HY, and other commercial catalysts also agreed well with the results presented here.[2–5] However, Mordi et al.[7,10] reported that, when PE was cracked by HZSM-5 at 350°C in a sealed reaction vessel, C_1–C_3 volatile products dominated, olefin yields were small, and propane was the most abundant volatile product.[10] In contrast, we did not detect C_1 and C_2 products, olefins were significantly more abundant than paraffins, and C_3 hydrocarbons were found to be exclusively propene. Aguado et al.[6] also employed batch processing at 400°C to study the effects of HZSM-5 and MCM-41 on PE cracking. Unlike Mordi et al., they used nitrogen to flush volatile products into cryogenic traps. They detected olefins in greater yields than paraffins; this is consistent with the results presented here. At low polymer/catalyst ratios, Aguado et al. reported that aromatic yields were much greater for HZSM-5 than for MCM-41; this is also consistent with results presented here. Discrepancies between results reported by Mordi et al. and those reported here and by Aguado et al. may be explained by the fact that Mordi et al. employed static batch processing. During their 2-h heating period, initial volatile products were likely cracked by the catalyst to yield smaller products. The fact that their paraffin yields exceeded olefin yields was likely due to increased disproportionation resulting from the fact that volatiles were not isolated from polymer residue.

CONCLUSIONS

Trends in volatile paraffin/olefin ratios and alkyl aromatic yields observed when PE is cracked by aluminosilicate catalysts cannot be correlated with variations in catalyst acidity or pore size alone. Product-slate differences occur because relative rates of specific carbenium ion reactions are affected by the combined effects of catalyst acidity and pore size. *In situ* monitoring of volatile cracking products as a function of PE conversion provides more information regarding reaction pathways than can be obtained by an analysis of products collected in

traps. Repetitive-injection GC/MS analysis can be used to monitor specific volatile reaction products and generate species-specific evolution profiles, which provide information regarding the order in which volatile products are formed.

REFERENCES

1. A Collection of Solid Waste Resources: Fall 1999; EPA-530-C-99-002; Office of Solid Waste and Emergency Response, U.S. Environmental Protection Agency, U.S. Government Printing Office: Washington, DC, 1999.
2. Garforth, A. A.; Lin, Y.-H.; Sharratt, P. N.; Dwyer, J. Appl Catal A 1998, 169, 331.
3. Manos, G.; Garforth, A. A.; Dwyer, J. Ind Eng Chem Res 2000, 39, 1198.
4. Manos, G.; Garforth, A. A.; Dwyer, J. Ind Eng Chem Res 2000, 39, 1203.
5. Mertinkat, J.; Kirsten, A.; Predel, M.; Kaminsky, W. J Anal Appl Pyrolysis 1999, 49, 87.
6. Aguado, J.; Serrano, D. P.; Romero, M. D.; Escola, J. M. J Chem Soc Chem Commun 1996, 725.
7. Mordi, R. C.; Fields, R.; Dwyer, J. J Anal Appl Pyrolysis 1994, 29, 45.
8. Lin, R.; White, R. L. J Appl Polym Sci 1995, 58, 1151.
9. Ishihara, Y.; Nanbu, H.; Saido, K.; Ikemura, T.; Takesue, T. Polymer 1992, 33, 3482.
10. Mordi, R. C.; Dwyer, J.; Fields, R. Polym Degrad Stab 1994, 46, 57.
11. Garforth, A. A.; Fiddy, S.; Lin, Y.-H.; Ghanbari-Siakhali, A.; Sharratt, P. N.; Dwyer, J. Thermochim Acta 1997, 294, 65.
12. Uemichi, Y.; Hattori, M.; Itoh, T.; Nakamura, J.; Sugioka, M. Ind Eng Chem Res 1998, 37, 867.
13. Sharratt, P. N.; Lin, Y.-H.; Garforth, A. A.; Dwyer, J. Ind Eng Chem Res 1997, 36, 5118.
14. Park, D. W.; Hwang, E. Y.; Kim, J. R.; Choi, J. K.; Kim, Y. A.; Woo, H. C. Polym Degrad Stab 1999, 65, 193.
15. Uemichi, Y.; Nakamura, J.; Itoh, T.; Sugioka, M.; Garforth, A. A.; Dwyer, J. Ind Eng Chem Res 1999, 38, 385.
16. Lin, Y.-H.; Sharratt, P. N.; Garforth, A. A.; Dwyer, J. Energy Fuels 1998, 12, 767.
17. Negelein, D. L.; Bonnet, E.; White, R. L. J Chromatogr Sci 1999, 37, 263.
18. Arauer, R. J.; Kensington, M.; Landolt, G. R. U.S. Pat. 3,702,886 (1972).
19. Schimdt, R.; Akporiaye, D.; Stocker, M.; Ellestad, O. H. J Chem Soc Chem Commun 1994, 1493
20. Kresge, C. T.; Leonowicz, M. E.; Roth, W. J.; Vartuli, J. C.; Beck, J. S. Nature 1992, 359, 710.
21. Tanev, P. T.; Pinnavaia, T. J. Chem Mater 1996, 8, 2068.
22. Beck, J. S.; Vartuli, J. C.; Roth, W. J.; Leonowicz, M. E.; Kresge, C. T.; Schmitt, K. D.; Chu, C. T. W.; Olson, D. H.; Sheppard, E. W.; McCullen, S. B.; Higgins, J. B.; Schlenker, J. L. J Am Chem Soc 1992, 114, 10824.
23. Bonnet, E. Ph.D. Dissertation, University of Oklahoma, 2000.
24. Wojciechowski, B. W. Catal Rev Sci Eng 1998, 40, 209.
25. Cumming, K. A.; Wojciechowski, B. W. Catal Rev Sci Eng 1996, 38, 101.